

## Analysis of Porous Silicon Formation on N-type Si (100) using Laser-Assisted Electrochemical Anodization Method

Risa Suryana\* and Nabia Qurrota Aini

Department of Physics, Faculty of Mathematics and Natural Sciences, Sebelas Maret University, Surakarta, Indonesia

\*Corresponding author: [rsuryana@staff.uns.ac.id](mailto:rsuryana@staff.uns.ac.id)

### ARTICLE INFO

#### Article history:

Received: 2 November 2021

Accepted: 16 February 2022

Available online: 27 May 2022

#### Keywords:

Porous silicon (PSi)

Electrochemical anodization

Illumination

Chemical bonding

N-type Si (100)

### ABSTRACT

Porous silicon (PSi) was formed on n-type Si (100) substrates using the laser-assisted electrochemical anodization method. The silicon surface was anodized in the solution of HF (40%) and ethanol (99%) in a ratio of 3:1 at a current density of 20 mA/cm<sup>2</sup> for 15 min. The laser was illuminated on a silicon surface during the etching process. PSi surface morphology was characterized by SEM and identification of chemical bonds using FTIR. The highest number of pores, the best pore size homogeneity, and the smallest pore diameter in PSi were formed in Si which was illuminated by a green laser (2.33 eV). In contrast to red (1.91 eV) and purple (3.06 eV) formed irregular pores because of their small number and inhomogeneous size. On the PSi surface, Si-H and Si-O-Si bonds are formed. The number of Si-Hn and Si-O-Si bonds is directly proportional to the number of pores formed in PSi.

### 1. Introduction

Porous silicon (PSi) is a promising material because it has excellent mechanical and thermal properties [1]. Although PSi has developed rapidly, many challenges apply PSi in electrical or optical devices. PSi in its application is used as anode in lithium-ion batteries [2], as fuel cells [3], plays a role in the development of biology and health [4], for drug delivery [5], till as superconducting electrodes [6].

Electrochemical anodization is most often used to manufacture PSi due to its straightforward process. The differences in the morphological characteristics of PSi can be influenced by doping density, anodization time, current density, and irradiation during the etching process. Various kinds of morphology and dimensions of the pores will provide a very diverse structure, mechanical, optical, electrical, thermal, emissive, physiochemical, and biochemical properties [7]. Parameters that can be used to distinguish morphological characteristics from one another include the percentage of porosity, the growth rate of pores, valence breaking, and pore diameter size [8].

In the previous study, we have succeeded in forming porous silicon on n-type Si (100) [9] and p-type Si (100) [10] with a variety of alcohol solutions using the electrochemical anodization method, and over n-type Si (100) and Si (111) substrates with significant variations of current [11]. To assist in PSi formation, silicon wafer was immersed in HF solution under illumination of coherent and incoherent light sources [12-18] such as laser, Xe lamps, and W lamps. Illumination was needed to get enough additional

holes to conduct the etching process in corrosion reaction. Additional holes can only be generated if the illumination uses light with energy higher than the silicon bandgap (1.12 eV) [18].

Xu and Adachi [12] used a Xe lamp to obtain the formation of large PSi layers on n-type Si(100) with a resistivity range of 1-3 Ω.cm, and Volovlikova et al. [13] studied the influence of illumination intensity on the silicon dissolution rate using a halogen lamp. They used p-type Si(100) with resistivity of 0.01, 1, and 12 Ω.cm. They concluded that the dissolution rate is directly proportional to the illumination intensity and inversely proportional to the wafer resistivity. On the other hand, Koker and Kolasinski [14] studied reaction kinetics and mechanistic implication on the formation of PSi in n-type Si(111) (4.5-6.4 Ω.cm) assisted by He-Ne laser (633 nm). Hadi et al. [15] fabricated PSi prepared by photo-electrochemical etching on HF:ethanol solution under 650 nm laser illumination. They conducted n-type Si(111) with a resistivity of 10 Ω.cm. Using Nd-YAG laser (1,064 nm) illumination on p-type Si(111) with a resistivity of 10 Ω.cm during the etching process, Ismail and Abood [16] found that responsivity, detectivity, and carrier lifetime of PSi dependent on the laser fluence.

Furthermore, a laser with 405 nm was used to obtain PSi on n-type Si [17]. It is revealed that porous structures depend on the potency of the laser. However, to the best of our knowledge, research on the effect of laser illumination variation during etching on the morphology and properties of PSi is still rare. This research will discuss the effect of laser illumination variations on the formation of PSi on the

n-type Si (100) surface using the electrochemical anodization method. The pore diameter average and the pore density of PSi are calculated from Scanning Electron Microscope (SEM) images using the ImageJ software. At the same time, Attenuated Total Reflection-Fourier Transform Infrared (ATR-FTIR) spectroscopy determines the chemical bonds on PSi.

## 2. Methods

Figure 1 is a schematic of a laser-assisted electrochemical anodization setup for the synthesis of PSi. N-type Si (111) substrates with a resistivity of 1-5  $\Omega\cdot\text{cm}$  were used to form PSi. First, the substrate was cut in 1 cm  $\times$  1.5 cm size then washed with acetone solution using the ultrasonic cleaner. Next, the substrate was dried with  $\text{N}_2$  gas. The silicon surface was etched in a solution of HF (40%) and ethanol (99%) in a ratio of 3: 1 at a constant current density of 20  $\text{mA}/\text{cm}^2$  for 15 min. A laser was illuminated directly on the center of the silicon surface during the anodization process. The laser color varied, i.e., red (650 nm), green (532 nm), and purple (405 nm), correlating 1.91 eV, 2.33 eV, and 3.06 eV, respectively. Platinum (Pt) was used as a cathode, while Si was used as an anode. After the etching process, the PSi is rewashed using acetone solution and then dried with  $\text{N}_2$  gas. The PSi samples were then characterized using SEM and ATR-FTIR spectroscopy.

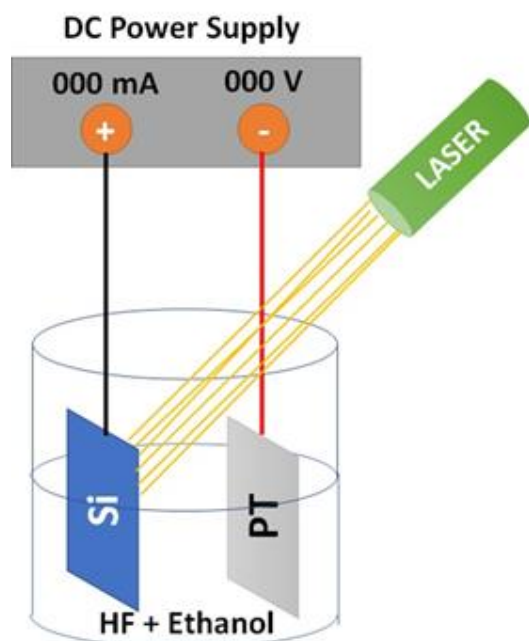


**Fig.1:** Schematic of laser-assisted electrochemical anodization setup for the synthesis of PSi.

## 3. Results and Discussion

Figure 2 depicts the morphology of PSi surfaces when a laser illuminates Si with the energy of 1.91 eV (red), 2.33 eV (green), and 3.06 eV (purple). Due to all the laser energy being higher than the bandgap energy of Si when Si absorbs the laser energy, electrons on the valence band will excite to the conduction band leaving the holes on the valence band [19]. These holes will

assist in breaking Si-H and Si-Si bonds by  $\text{F}^-$  ions to form pores [20].

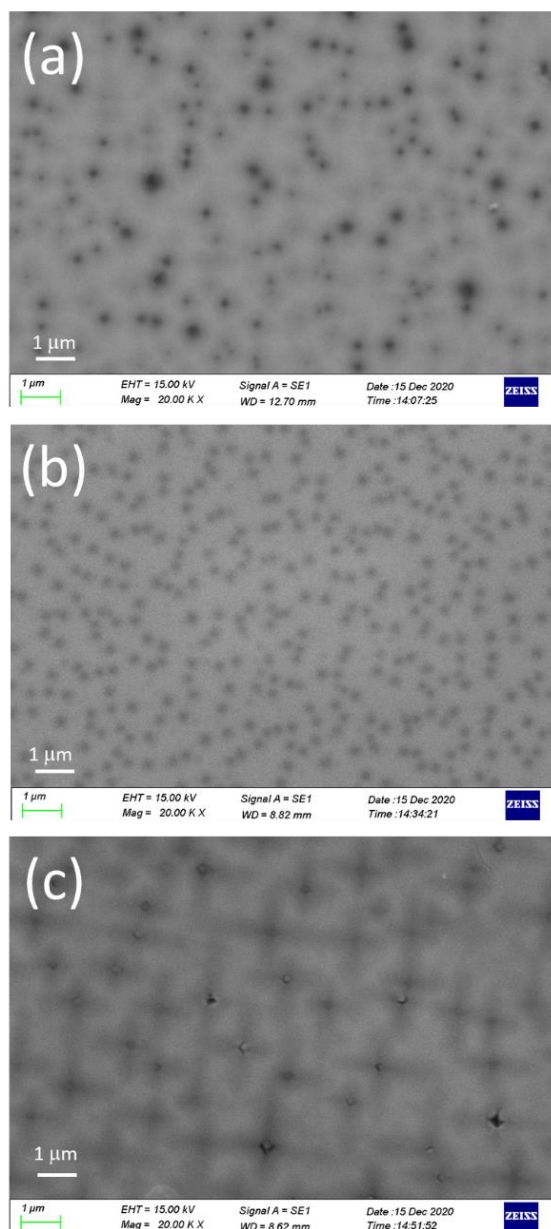


**Fig. 2:** Morphology of PSi surfaces illuminated during etching process by laser energy of a) 1.91 eV (red), b) 2.33 eV (green) and c) 3.06 eV (purple).

The black color of SEM images, as shown in Fig. 2, indicates pores on Si surfaces. Pores distribution for each laser illumination treatment reveals that using the green laser [sample (b)] during the etching process is more homogenous than using red [sample (a)] and purple laser [sample (c)]. As a result, the pore size and pore shape are almost similar. On the contrary, sample (a) shows a pore-like structure while sample (c) shows a cross-like structure. The previous study obtained pore-like and cross-like structures when n-type Si (100) surfaces were etched using 10  $\text{mA}/\text{cm}^2$  for 10-20 min and 30 min, respectively [9]. Alwan et al. [21] explained that under violet illumination, the porosity forms a side branch that creates the side branch that propagates

perpendicularly to their primary development path, forming a cross-like structure.

Figure 3 shows the pore density and pore diameter average of P*Si* after the different laser illuminates Si surfaces. Amount pores are calculated in an area constant of  $13.65 \mu\text{m} \times 10.24 \mu\text{m}$ , as shown in Fig. 2. Thus, the pore density of P*Si* under green illumination is higher than red and purple illumination. This value is reasonable because the average pore diameter of P*Si* under green illumination is the smallest.

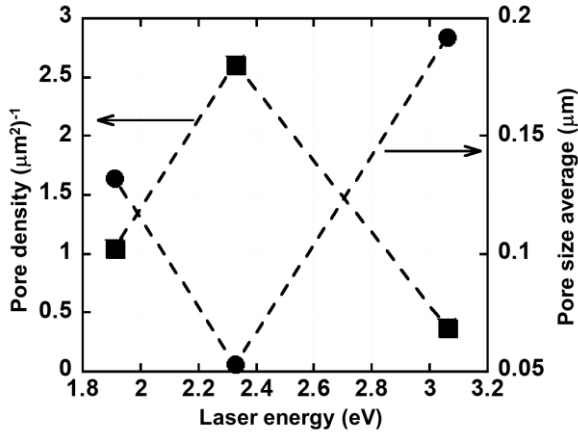


**Fig. 3:** Pore density and pore diameter average of P*Si* for different laser energy.

Holes generation is directly proportional to the number of photons absorbed in silicon, and during chemical etching, the bond exchange coincides between the molecules in solution and Si atoms on surfaces [22]. Furthermore, the hole enters the Si interface and electrolytes [23].

Based on the distribution and the density of P*Si*, it is considered that under the illumination of the laser on the Si surfaces during the etching process, the green laser energy is absorbed by Si to produce hole density and simultaneously diffuses to the Si surface for the P*Si* formation process. The green laser illumination encourages the corrosion reaction in the etching process to take place smoothly and regularly. Meanwhile, under the red laser illumination, it is considered that fewer holes are produced, which causes holes to diffuse irregularly and not simultaneously. As a result, the corrosion reaction of the Si surfaces cannot run smoothly, resulting in the pore-like structure being inhomogeneous, including large and small diameters appearing on the Si surface. In the case of the purple illumination, we assume too many holes are generated then diffuse to the Si surface in out-of-control conditions.  $\text{F}^-$  ions break Si-H and Si-Si bonds very fast, and the direction of corrosion is vertical and horizontal, resulting in P*Si* in a cross-like structure.

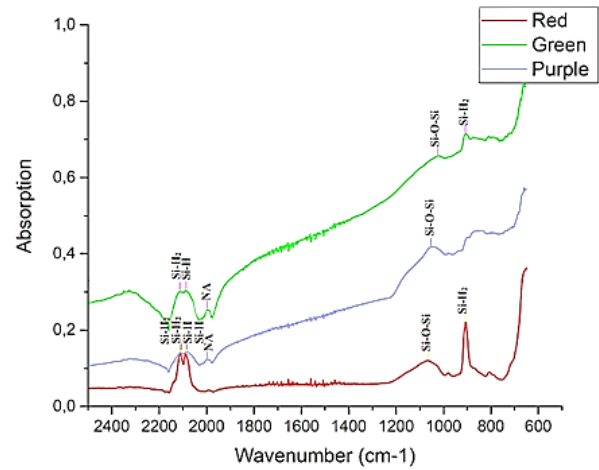


**Fig. 4:** FTIR spectrum graph of absorption band intensity on P*Si* for different the laser energy illuminated during the etching process.

Figure 4 is the FTIR spectrum of absorption band intensity on P*Si* in the wavenumber range of 600-2500  $\text{cm}^{-1}$  for each laser energy, i.e., red, green, and purple. The absorption peaks are dominated by Si-H<sub>n</sub> and only one peak owing Si-O-Si. However, there is an NA peak at a wavenumber of 1997  $\text{cm}^{-1}$ . The absorption peaks that appear in FTIR measurements indicate the presence of a specific bond in P*Si* [24].

**Table 1.** Summary of wavenumber, chemical bond, and vibration mode of P*Si* illuminated by (a) red, (b) green, and (c) purple laser.

	Wavenumber (cm <sup>-1</sup> )	Bonds	Vibration Mode
(a)	2113,2089	Si-H <sub>2</sub> ,Si-H	Stretch
	1066	Si-O-Si	Stretch Antisymmetric
	980	Si-O-Si	Stretch Antisymmetric
	905	Si-H <sub>2</sub>	Deformation Symmetric
(b)	2111,2089	Si-H <sub>2</sub> ,Si-H	Stretch
	1997	NA	NA
	1021	Si-O-Si	Stretch Antisymmetric
	905	Si-H <sub>2</sub>	Deformation Symmetric
(c)	2107,2083	Si-H <sub>2</sub> ,Si-H	Stretch
	1997	NA	NA
	1043	Si-O-Si	Stretch Antisymmetric

Absorption of P*Si* is highest when the green laser illuminates the Si compared to using the red and purple laser. Regarding pore density and pore size, the P*Si* obtained by green illumination has the P*Si* surface area higher than red or purple laser-illuminated during the etching process [25]. However, the pore absorption resulting from the purple laser illumination is higher even though it has a lower density than the red laser. It is due to not only the pore-like structure that absorbs photons, but also the cross-like structure.

Table 1 summarizes the wavenumber, bonds, and vibration mode of P*Si* for each illumination of the red,

green, and purple laser. This PSi obtained from the green laser has the highest absorption intensity because it has the highest pore density and the most significant area increase. The increase in area in PSi makes it have a broader area to undergo oxidation so that there are many Si-O-Si bonds. In addition, the number of Si-H bonds is because the Si-H bond is a susceptible bond to the degree of sample oxidation. This phenomenon is shown when one or more oxygen atoms are bonded to the surface silicon atoms containing one or more hydrogen atoms; the Si-H vibrations shift to a higher frequency [26].

#### 4. Conclusion

Porous silicon (PSi) has been formed on n-type Si(100) using the laser-assisted electrochemical anodization method. The homogenous and highest density of PSi was obtained by using the green laser during the etching process. As a result, the pore shape is pore-like and cross-like structures when using the red or green and purple laser. In addition, the absorption peak of PSi using the green laser is higher than using the red and the purple laser. Therefore, the formation of PSi assisted the green laser in anodization electrochemical is very promising in applying optical devices.

#### 5. Conflict of Interest

The authors declare that they have no conflict of interest.

#### Acknowledgements

Authors would like to thank RKAT PTNBH Universitas Sebelas Maret 2021 for financial support through Skema Penelitian Unggulan Terapan UNS (PUT-UNS) with Contract No. 260/UN27.22/HK.07.00/2021.

#### References

- [1] E. X. Perez, *Design, Fabrication and Characterization of Porous Silicon Multilayer Optical Devices*, (Universiat Rovira I Virgili, Tarragona, 2007).
- [2] M. Thakur, M. Issacson, S. L. Sinsabaugh, M. S. Wong, and S. L. Biswal, "Gold-coated Porous Silicon Films as Anodes for Lithium Ion Batteries," *J. Power Sources*, 205, 426-432, (2012).
- [3] M. Jaouadi, W. Dimassi, M. Gaidi, R. Chtourou, and H. Ezzaouia, "Nanoporous Silicon Membrane for Fuel Cells Realized by Electrochemical Etching," *App. Surf. Sci.*, 258, 15, 5654-5658 (2011).
- [4] O. I. Ksenofontovaa, A. V. Vasina, V. V. Egorova, A. V. Bobyl'b, F. Y. Soldatenkovb, E. I. Terukovb, V. P. Ulinb, N. V. Ulinb, and O. I. Kiseleva, "Porous Silicon and Its Applications in Biology and Medicine," *Tech. Phys.*, 59, 1, 66-77, (2014).
- [5] E. Nekovik, J. S. Catherine, A. Kaplan, W. Theis, and L. T. Canham, *A Gentle Sedimentation Process for Size-Selecting Porous Silicon Microparticles to be Used for Drug Delivery Via Fine Gauge Needle Administration*, (Springer Publisher, 2020).
- [6] V. V. Bolotov, S. N. Nesov, E. V. Ponomareva, K. E. Knyazef, Y. A. Ivlev, Stenkin, and V. E. Roslikov, "The Formation of Nanocomposites Carbon Nanotubes/Porous Silicon for Supercapacitor Electrodes," *AIP Conf. Proc.*, 2310, 1, (2020).
- [7] V. Lehmann, R. Stengl, and A. Luigart, "On the Morphology and The Electrochemical Formation Mechanism of Mesoporous Silicon," *Mat. Sci. Eng.*, 69, 70, 11-22, (2000).
- [8] F. Karbassian, *Porous Silicon*, (Intechopen Publication, 2018).
- [9] R. Suryana, D. K. Sandi, and O. Nakatsuka, "The Morphological Study of Porous Silicon Formed by Electrochemical Anodization Method," *IOP Conf. Ser.: Mater. Sci. Eng.*, 333, 1, 012030, (2018).
- [10] S. Wijayanti, Sehati, and R. Suryana, "The Formation of Porous Silicon (PSi) on P-type Si(100) Substrate via the Electrochemical Anodization Method with Varying Current Density," *J. Phys.: Conf. Ser.*, 1825, 1, 012068, (2021).
- [11] B. Pratama, I. Syahidi, E. Prayogo, Khairurrijal, K. Triyana, H. Susanto, and R. Suryana, "Formation of Porous Silicon on N-type Si (100) and Si (111) Substrates by Electrochemical Anodization Method," *Mater. Today: Proc.*, 44, 3426-3429, (2021).
- [12] Y. K. Xu, and S. Adachi, "Light-Emitting Porous Silicon Formed by Photoetching in Aqueous HF/KIO<sub>3</sub> Solution," *J. Phys. D: Appl. Phys.*, 39, 4572-4577, (2006).
- [13] O. Volovlikova, S. Gavrillov, and P. Lazarenko, "Influence of Illumination on Porous Silicon Formed by Photo-Assisted Etching of p-Type Si with a Different Doping Lever," *Micromachines*, 11, 199, (2020).
- [14] L. Koker, and K. W. Kolasinski, "Laser-Assisted Formation of Porous Si in Diverse Fluoride Solution: Reaction Kinetics and Mechanistic Implication," *J. Phys. Chem. B*, 105, 3864-3871, (2001).
- [15] H. A. Hadi, R. A. Ismail, and N. F. Habubi, "Fabrication and Characterization of Porous Silicon Layer Prepared by Photo-Electrochemical Etching in CH<sub>3</sub>OH:HF Solution," *Int. Lett. Chem. Phys. Astron.*, 8, 29-36, (2013).
- [16] R. A. Ismail, and M. K. Abood, "Effect of Nd:YAG Laser Irradiation on the Characteristics of Porous Silicon Photodetector," *Int. Nano. Lett.*, 3, 11, (2013).
- [17] F. S. Carrillo, V. L. Gayou, G. G. Salgado, R. D. Macuil, and N. C. Ramirez, "Structural Properties of Porous Silicon Obtained with Laser Photoetching Assisted by Computerized Numeric Control," *J. Laser Appl.*, 33, 022001, (2021).
- [18] J. Jakubowicz, "Nanoporous silicon fabricated at different illumination and electrochemical

- conditions," *Superlattices and Microstructures*, 41, 205–215, (2007).
- [19] S. Z. Sze and K. N. Kwok, *Physics of Semiconductor Devices*, (John Wiley & Sons, 2007).
- [20] V. Lehmann and U. Gosele, "Porous Silicon Formation: A Quantum Wire Effect," *App. Phys. Lett.*, 58, 856, (1991).
- [21] M. A. Alwan, A. A. Abbas, and A. B. Dheyab, "Study the Characteristic of Planner and Sandwich PSi Gas Sensor (Comparative Study)," *Silicon*, 10, 2527-2534, (2018).
- [22] V. Lehmann and H. Foll, "Formation Mechanism and Properties of Electrochemically Etched Trenches in N-Type Silicon," *J. Electrochem. Soc.*, 137, 2, 653-659, (1990).
- [23] L. Koker and K. W. Kolasinski, "Photo-electrochemical Etching of Si and Porous Si in Aqueous HF," *Phys. Chem. Chem. Phys.*, 2, 277-281, (2000).
- [24] Y. H. Ogata, *Characterization of Porous Silicon by Infrared Spectroscopy*, in *Handbook of Porous Silicon*, Leigh Canham Editor, 2<sup>nd</sup> ed. (Springer International Publishing AG, part of Springer Nature, 2018).
- [25] D. B. Mawhinney, J. A. Glass, and J. T. Yates, "FTIR Study of the Oxidation of Porous Silicon," *J. Phys. Chem. B*, 101, 1202-1206, (1997).
- [26] M. J. Sailor, *Porous Silicon in Practice: Preparation, Characterization, and Applications*, (Wiley-VCH Publisher, Weinheim, 2011).